

Directional light beaming control by a subwavelength asymmetric surface structure

Ding-Zheng Lin¹, Tsung-Dar Cheng¹, Chin-Kai Chang¹, Jyi-Tyan Yeh², Jonq-Min Liu²
Chau-Shioung Yeh¹, *Chih-Kung Lee^{1,3}

¹ Institute of Applied Mechanics, National Taiwan University, Taipei, Taiwan

² Industrial Technology Research Institute, Material and Chemical Research Laboratories, Hsinchu, Taiwan

³ Department of Engineering Science & Ocean Engineering, National Taiwan University, Taipei, Taiwan

*cklee@mems.iam.ntu.edu.tw

Abstract: We propose a direct experimental set-up to observe the directional beaming effect of surface plasmon. A single diffracted beam from an asymmetric-sided surface corrugation is demonstrated. A single subwavelength slit with an asymmetric structure was fabricated using a focused ion beam (FIB) onto a metal surface with a glass substrate. By means of surface plasmon (SP) diffraction, the directionality of the light can be changed by the period of the metallic gratings. We show corresponding numerical simulations achieved by a Rigorous Coupled-Wave Analysis (RCWA) method and a Finite-Difference Time-Domain (FDTD) method. The simulation results were in agreement with the experimental data.

©2007 Optical Society of America

OCIS codes: (240.6680) Surface plasmons; (050.1950) Diffraction gratings; (240.0240) Optics at surfaces.

References and links

1. H. J. Lezec, A. Degiron, E. Devaux, R. A. Linke, L. Martin-Moreno, F. J. Garcia-Vidal, and T. W. Ebbesen, "Beaming light from a subwavelength aperture," *Science* **297**, 820-822 (2002).
2. C. T. Wang, C. L. Du, Y. G. Lv, and X. G. Luo, "Surface electromagnetic wave excitation and diffraction by subwavelength slit with periodically patterned metallic grooves," *Opt. Express* **14**, 5671-5681 (2006). <http://www.opticsexpress.org/abstract.cfm?id=90329>
3. L. Martin-Moreno, F. J. Garcia-Vidal, H. J. Lezec, A. Degiron, and T. W. Ebbesen, "Theory of highly directional emission from a single subwavelength aperture surrounded by surface corrugations," *Phys. Rev. Lett.* **90**, 167401 (2003).
4. F. J. Garcia-Vidal, L. Martin-Moreno, H. J. Lezec, and T. W. Ebbesen, "Focusing light with a single subwavelength aperture flanked by surface corrugations," *Appl. Phys. Lett.* **83**, 4500-4502 (2003).
5. J. Bravo-Abad, F. J. Garcia-Vidal, and L. Martin-Moreno, "Wavelength de-multiplexing properties of a single aperture flanked by periodic arrays of indentations," *Photon. Nanostruct.* **1**, 55-62 (2003).
6. L. B. Yu, D. Z. Lin, Y. C. Chen, Y. C. Chang, K. T. Huang, J. W. Liaw, J. T. Yeh, J. M. Liu, C. S. Yeh, and C. K. Lee, "Physical origin of directional beaming emitted from a subwavelength slit," *Phys. Rev. B* **71**, 041405 (2005).
7. A. I. Fernandez-Dominguez, E. Moreno, L. Martin-Moreno, and F. J. Garcia-Vidal, "Beaming matter waves from a subwavelength aperture," *Phys. Rev. A* **74**, 021601(R) (2006).
8. H. Caglayan, I. Bulu, and E. Ozbay, "Plasmonic structures with extraordinary transmission and highly directional beaming properties," *Microw. Opt. Technol. Lett.* **48**, 2491-2496 (2006).
9. D. Z. Lin, C. K. Chang, Y. C. Chen, D. L. Yang, M. W. Lin, J. T. Yeh, J. M. Liu, C. H. Kuan, C. S. Yeh, and C. K. Lee, "Beaming light from a subwavelength metal slit surrounded by dielectric surface gratings," *Opt. Express* **14**, 3503-3511 (2006). <http://www.opticsexpress.org/abstract.cfm?id=89340>
10. T. Thio, K. M. Pellerin, R. A. Linke, H. J. Lezec, and T. W. Ebbesen, "Enhanced light transmission through a single subwavelength aperture," *Opt. Lett.* **26**, 1972-1974 (2001).
11. C. K. Lee, C. L. Lin, D. Z. Lin, T. D. Cheng, C. K. Chang, L. B. Yu, and C. S. Yeh, "Developing a nanowriter system: Simulation and experimental set-up of a plasmonic-based lens design," *Mater. Sci. Forum* **505-507**, 1-6 (2006).
12. D. McGloin, and K. Dholakia, "Bessel beams: diffraction in a new light," *Contemp. Phys.* **46**, 15-28 (2005).
13. S. Shinada, J. Hashizume, and F. Koyama, "Surface plasmon resonance on microaperture vertical-cavity surface-emitting laser with metal grating," *Appl. Phys. Lett.* **83**, 836-838 (2003).

14. J. Hashizume, and F. Koyama, "Plasmon enhanced optical near-field probing of metal nanoaperture surface emitting laser," *Opt. Express* **12**, 6391-6396 (2004). <http://www.opticsexpress.org/abstract.cfm?id=82005>
15. J. Hashizume, and F. Koyama, "Plasmon-enhancement of optical near-field of metal nanoaperture surface-emitting laser," *Appl. Phys. Lett.* **84**, 3226-3228 (2004).

1. Introduction

According to the diffraction theory, light transmitted through a subwavelength slit will diffract in all directions. Recently, it was found that when a subwavelength hole is surrounded by a symmetric surface structure, the radiating beam can be confined to a small angle [1]. This directional beaming phenomenon has been analyzed theoretically [2-5] and experimentally [6] by various research groups. The feasibility of this concept has also been demonstrated to apply to matter waves [7] and microwaves [8]. In our previous work [6,9], performed under white light illumination, we found that when a light beam is diffracted along a negative beaming angle in a symmetric-sided surface structure, the light beam diffracted from each side will interfere with each other. As shown in Fig. 1, the observed colors of the image can be defined as the superposition of different wavelengths. Therefore, the color we see may not correspond to an actual single wavelength (i.e. an observed yellow (Y) may be yellow or it may be a mix of red (R) and green (G)). In this letter, we propose a direct experimental set-up to observe the negative beaming angles. The influences of the grating period and depth will be addressed.

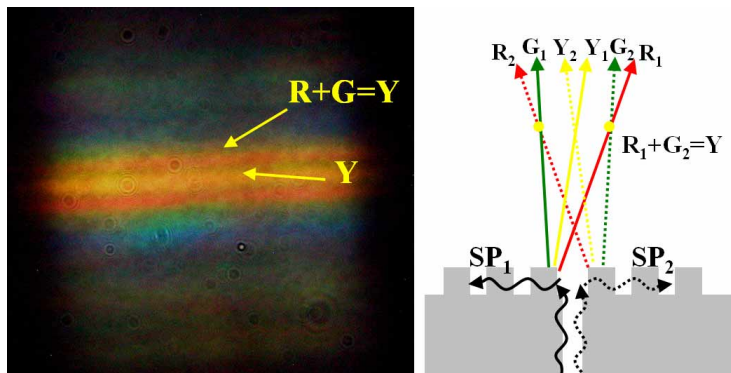


Fig. 1. Observed colors as a result of the superposition of negative beaming angles of the symmetric-sided surface structure. (Note: the suffix 1 and 2 represent the SP diffraction from a left and right side, respectively)

2. Simulations

In order to understand the directional beaming of the asymmetric-sided structure (AS structure), Fig. 2(a), a FDTD method was applied to determine the directionality of these structures. The grating depth (d) of the AS structures was set at 60nm, and the grating period (p) with filling factor 0.5 was set at 400nm, 450nm, 500nm, 550nm, 600nm, and 650nm respectively. The silver film thickness (t) was set at 250nm, slit width (w) at 130nm, and the dielectric constant of the silver was determined by a Drude model. The wavelength (λ) of the p -polarized light source was 633nm at normal incidence from the back side. The number of grooves in the simulations was set at 10. The angles of the directional emission are defined in Fig. 2(b). If the direction of the wave vector projection (k_x) is the same as the direction of the surface plasmon wave vector (k_{sp}), the beaming angle can be defined as a positive angle. For the opposite case, the beaming angle can be defined as a negative angle.

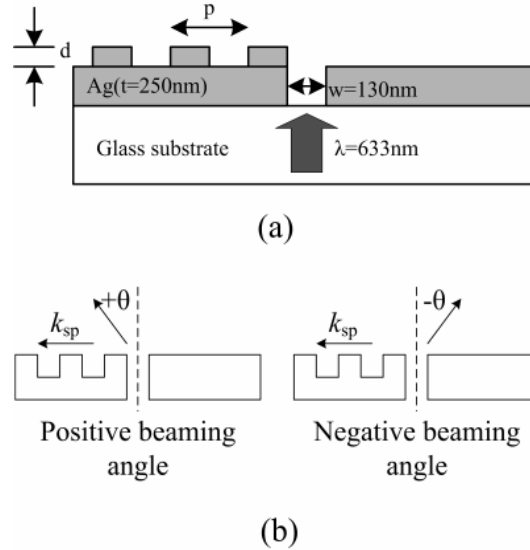


Fig. 2. (a) Schematic of an asymmetric-sided (AS) structure used in the simulations; (b) Definition of a positive (left) and negative (right) directional beaming angle.

Figure 3(a) shows the FDTD simulation results for different periods of the AS structure with 60nm groove depths and 633nm incident wavelength. As expected, we found that the beaming angles changed with the different periods at a given wavelength. Like a symmetric-sided structure, the exiting beam from the AS structure also had directionality. In addition to the period of the surface structure, the depth of the surface structure also plays an important role [10]. In order to check the consistency between our simulated and experimental data, the limits of the fabrication precision needed to be taken into consideration. We know that the FIB system allows good control of the periodicity, but it is much harder to mill the depth of the grating precisely. Figure 3(b) shows the simulation results for a 500nm period grating with different grating depths ranging from 50nm to 100nm. It is clear from Fig. 3(b) that when the grating depth is deep, the beaming angle will be broad. In addition, the diffraction efficiency also changes when the grating depth varies. In our data, the efficiency of the main beaming angle (near zero degrees) gradually increased and reached a maximum at a grating depth of 70nm, and then decreased at larger grating depths. The beaming is a result of an interference phenomenon of the surface waves generated at the interface under appropriate conditions [3]. Firstly, the output evanescent beam diffracts from the central slit into a vacuum and into the surface grooves. The waves in the grooves may diffract into the vacuum or into another groove. Secondly, the waves form a self-consistent distribution at the output surface. When the waves diffract into the grooves, the groove geometries will then influence the amplitude or phase of the excited surface electromagnetic (EM) waves [2] (i.e. the deeper the groove depth, the wider the diffraction angle due to the excitation of the surface EM modes localizing at a few grooves around the central slit)

According to the surface plasmon diffraction theory, the surface plasmon decoupled into light can be expressed by the following equation:

$$k_{sp} - i \frac{2\pi}{p} = k_0 \sin \theta \quad (1)$$

where k_0 is the wave vector of the diffracted light in free space, k_{sp} is the wave vector of the coupled surface plasmon, p is the grating period, θ is the beaming angle, and i is an integer. It is difficult to obtain an analytical solution as the wave vector of the coupled surface plasmon

is very difficult to derive. The RCWA method and the Helmholtz reciprocity theorem can be adopted to determine the beaming angles by calculating the reflection minimum from the output side [6]. As shown in Fig. 4(a), when light impinges on the reflection grating and we change the incident angle, we can obtain an angle where the minimum reflection occurs, which means that the energy of incident light is transferred to the surface plasmon resonance field. On the contrary, if there is a surface plasmon resonance field on the asymmetric-sided structure, based on the energy conservation of the whole grating system we can use the Helmholtz reciprocity theorem to predict the beaming angles reversely. The simulation results in Fig. 4(b) show that the beaming angles change with the periods. Comparing the results shown in Fig. 4(b) and Fig. 3(a), it is clear that the results calculated by the FDTD and RCWA methods reflect the same trend.

The results shown in Fig. 4(b) depict some peculiarity for the output data at zero degrees which can be attributed to a truncation of the output data. As a RCWA method was used to solve the optical diffraction problem of the periodic structure, the left and right boundary repeats the simulation domain into infinite space. Therefore, the output data from the RCWA method cannot distinguish the sign of the incident angles. More specifically, the RCWA can only show the diffraction efficiency from 0 to 90 degrees. In order to recognize whether the beaming angle is positive or negative, we can change slightly the grating period. From Eq. (1), we can see that increasing the grating period leads to a decrease of the modulation wave vector ($2\pi/p$) of the surface plasmon involved. When we increase the grating period, and if the beaming angle is also increased, the angle is then deemed positive. If we increase the grating period and it leads to a decrease in the beaming angle, the angle will be deemed negative.

3. Experimental Set-up

To demonstrate the beaming properties of asymmetric-sided structures, a series of visual experiments was performed. The geometries of the samples were fabricated according to the same parameters as those used in the simulations in order to check the consistency between the simulated data and experimental data. First, silver film of 250nm thickness was evaporated onto a 500 μ m glass substrate. Then, the AS surface gratings and a slit were fabricated using a FIB system (FEI, Nova 200). An atomic force microscope (AFM) was applied to determine the geometry after fabrication. The grating periods were measured with the AFM which confirmed that the accuracy of the fabrication was the same as the original design. However, our analysis found that the variations of the grating depths were found to be around 10nm (60 ± 10 nm). This slight variation in the grating depth could be the result of fabrication errors or errors induced by the image scanning process using the FIB system. Since the depth could not be controlled very precisely, the influence of the depth variation was taken into consideration by performing the simulations as shown in Fig. 3(b).

The experimental set-up for observing the directional beaming included an inverted optical microscope (Olympus, IX71), which was equipped with a halogen light source, and a polarizer. The collection angle of the objective (20X, NA=0.5) was 53.2 degrees. In order to obtain the information of the beaming angles, a series of photos were taken with a CCD camera (Olympus, DP70) at different z-positions with respect to the focal plane. The optical images obtained are shown in Fig. 5, where the grating periods varied from 400nm to 650nm. In Fig. 5, the dashed line indicates the position of the central slits. The surface gratings are situated at the upper plane of the dashed line. From the previous definition, the upper plane of the dashed line was a positive beaming angle, and the lower plane reflected a negative beaming angle. The pictures were taken by changing the focal plane of the objective lens every 10 μ m distance away from the output plane. From the picture, it is clear that at a distance of 30 μ m from the output plane, the beaming angle of the different grating periods are obviously distinct.

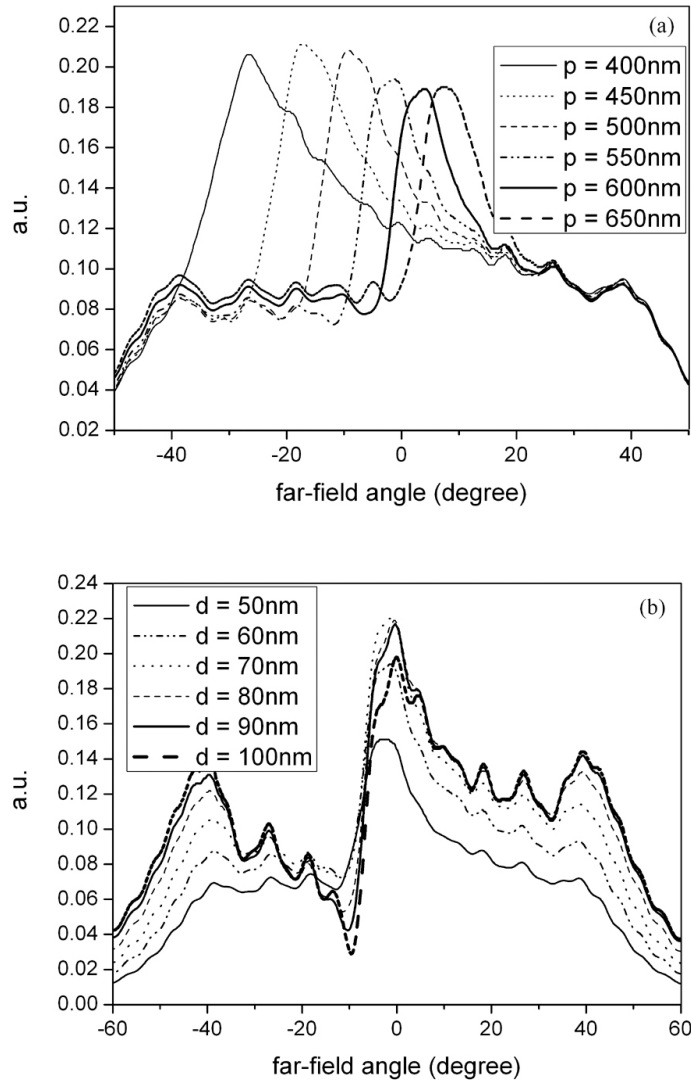


Fig. 3. (a) FDTD simulation results for different periods of the AS structures with 60nm groove depths and 633nm incident wavelength. The far-field angles (beaming angles) can be determined by the far-field calculations of the Poynting vector (S_z) at the output surface; (b) FDTD simulation results for different grating depths, which range from 50nm to 100nm for a 500nm grating period.

The period of the third structure from the left was set at 550nm, and the output beam was close to the central dashed line. Comparing these with the simulation results in Fig. 3(a) and Fig. 4(b), the beaming angle can be seen as also being close to zero degrees. Other grating periods in Fig 5 all demonstrate the same tendency as the simulation results in Fig. 3(a) and Fig. 4(b). We can also see that the surface plasmon diffraction only exists when the incident light is p -polarized (e.g. the electric field of the incident light is perpendicular to the groove direction). The last two frames in Fig. 5 compare the experimental results when the incident light is changed from a p -polarization to a s -polarization. If the incident light is p -polarized, the beaming effect is clear. It does not exist when the incident light is s -polarized which implies a relationship to the surface plasmon diffraction. We can calculate the beaming direction by utilizing a color filter (central wavelength 633nm and bandwidth 20nm). Following the inner and outer boundaries of the light beam, we can calculate the mean

beaming angle. The beaming angles obtained experimentally and by simulation are summarized in Table 1. The data shows good consistency between the simulated and experimental results.

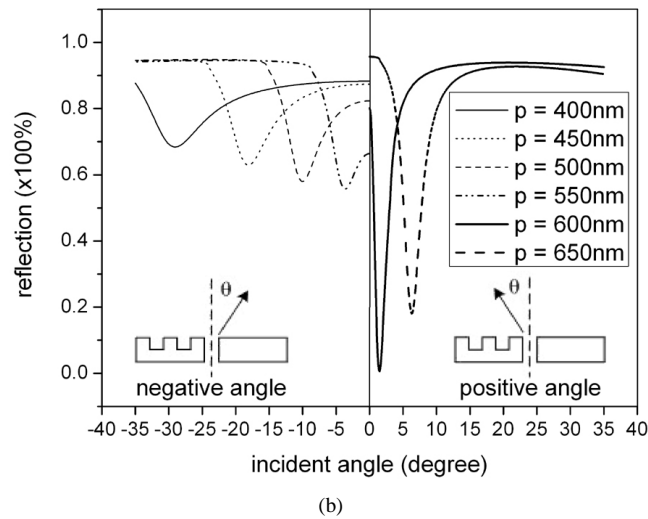
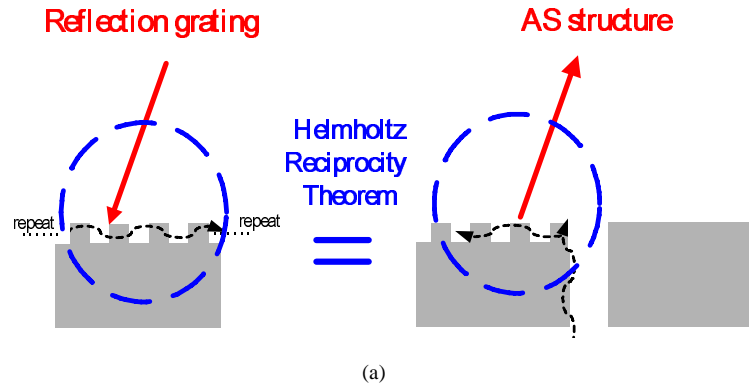


Fig. 4. (a) Concept of the Helmholtz reciprocity theorem; (b) RCWA simulation results for different periods of an AS structure (simulation conditions identical to that in Fig. 3(a)).

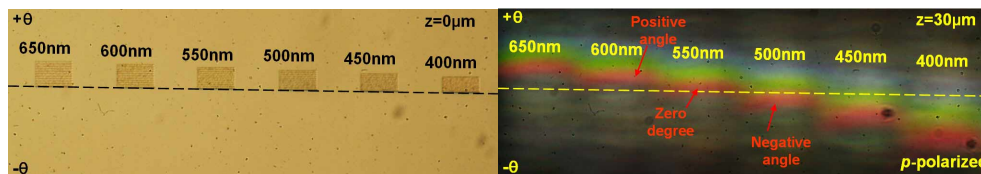


Fig. 5. (1.49MB) Movie of a beaming phenomenon at different z cross sections under white light illumination. Optical transmission image of an AS structure when the focal plane is on the surface (left) and at a distance of $30\mu\text{m}$ (right). The periods of the asymmetric-sided structure are in the range from 650nm to 450nm . The dashed line indicates the position of the central slit (zero degrees). The light beam polarizations are all p -polarized except the last one which is s -polarized. (The objective is $20\times$ with NA equal to 0.5)

Table 1. Experimental vs. simulation results of the beaming angle at incident wavelength equals to 633 nm.

Grating period (nm)	400nm	450nm	500nm	550nm	600nm	650nm
Experiment (deg)	-24.9	-13.7	-7	1.2	5.8	8.1
FDTD simulation (deg)	-26.3	-17.2	-9.3	-1	4	7.6
RCWA simulation (GSolver TM) (deg)	-29.7	-18.8	-10.5	-4	1.6	6.4

4. Discussion

In Table 1, we found a tendency for the simulated results to favor a more negative angle as compared to the experimental results. This tendency was more clearly depicted when the grating period was at 550nm, where the simulated and the experimental beaming angle showed a different sign. Several possible reasons can explain this situation. First, the grating depth used in the simulations was at 60nm, while the fabricated grating depth varied from 50nm to 70nm. This 10 nm grating depth variation could be the reason for the beaming angle variation as shown in Fig. 3(b) where the beaming angle can be seen to shift by 2 to 4 degrees. The beaming angle variance could also be the result of human error in misjudging the location of the central beam during the experimental set-up. As the bandwidth of the color filter was 20nm, it was difficult to judge the central wavelength directly. Although we minimized the error by measuring two boundaries of the beam to estimate the position of the central wavelength, the blur at the boundaries could also have contributed to some additional errors.

The directional beaming effect in the previous articles [9] can also be explained by this experimental set-up. If the surface structures are symmetric, each side will produce a single tiny beam at the output surface. By tuning to the appropriate grating period and groove width, the output beams will have a negative beaming angle. The two tiny beams emitted will then interfere to produce a smaller spot. The spot size and depth of focus can then be changed by choosing the two appropriate negative beams [11].

5. Conclusions

In this paper, we presented a subwavelength metal slit surrounded by asymmetric structures, both by simulation and by experimental set-up. We showed that the different periods will induce a single diffracted beam with different beaming angles. The surface plasmon diffraction theory can be applied to explain the directional beaming effect. The simulation and experimental data were in good agreement. The AS structures created the directional control of the surface plasmon and diffracted the energy to free space within the specific direction of the tiny beams which are an important basis to generate a quasi-Bessel beam [12]. The verification of the optical properties of the AS structures provide a path to pursue many industrial applications such as nanolithography, optical storage [13-15], optical communication [5], optical tweezers, etc.

Acknowledgments

We deeply appreciate the support of Professor T. W. Ebbesen and his colleagues at the Nanostructures Laboratory, University Louis Pasteur, France. The authors would also like to acknowledge the financial support from the Material & Chemical Research Laboratory of the Industrial Technology Research Institute (ITRI) and from the Taiwan National Science Council through Grants NSC 95-2221-E-002-122.